Robust NLOS Discrimination for Range-Based Acoustic Pose Tracking

Ferdinand Packi and Uwe D. Hanebeck

Intelligent Sensor-Actuator-Systems Laboratory (ISAS),
Institute for Anthropomatics,
Karlsruhe Institute of Technology (KIT), Germany.
ferdinand.packi@kit.edu, uwe.hanebeck@ieee.org

Abstract—**Indoor localization is a field in research with many competing technologies using different kinds of media. A common challenge faced by most systems is dealing with Non-Line-of-Sight (NLOS) conditions. We are addressing this issue with focus on sound in the frequency range above 20 kHz, as we encountered severe occurrence of outliers due to multipath propagation, by reflections, and from occlusion. The proper discrimination of erroneous signals is of special concern during initialization time of the tracking system. During run time, the computationally demanding process can be spared, if motion is modelled and stochastic filtering techniques are applied. This paper depicts solutions for both cases, and demonstrates that a combined use of static and dynamic localization methods delivers increased robustness at an affordable computational cost.**

I. INTRODUCTION

Indoor localization has become an emerging field in research since location-based services have aimed to hit the mass market. There is a demand for mobile, handheld devices to offer absolute geolocation in buildings similar to GPS. Also the gaming industry pushes on multimodal input, like the user's position and viewing direction, to spice up their products, like Microsoft's Kinect[TM]. But also services for the elderly, impaired, and blind people are on the list. Firefighter training and education, like evacuation scenarios, can be performed using a realistic, immersive telepresence system, which requires accurate and fluent positioning.

Unlike outdoor environments, where localization and tracking are covered by combinations of GPS and INS to a satisfactory extent, indoor positioning is still a demanding task, as it faces several additional challenges. Due to the smaller scale, as a matter of fact, accuracy in buildings needs to be better by at least two orders of magnitude compared to common navigation systems.

Optical systems as well as systems based on (ultra-) sound require line-of-sight (LOS) conditions. Although some approaches with low frequency sound have proven robustness against occlusions (thanks to diffraction), they still suffer from multipath propagation due to reflections from even surfaces such as walls or windows [1]. Radio and other (electro-) magnetic systems are strongly influenced by metal, which is prevailing in most modern buildings.

Despite the known issues concerning acoustic wave propagation, we chose to tackle the presence of Non-Line-of-Sight (NLOS) conditions, where common designs fail. This comes, of course, at the expense of redundancy in measurements, along with an increase in computation complexity.

Distance measurements are carried out by using Time-of-Flight (TOF) of characteristic, distinguishable sound packets

Fig. 1. User wearing the integrated tracking and visualization system. Vision is provided by an HMD, position and viewing direction are resolved according to the user's actual pose.

that are emitted concurrently by room-fixed beacons. Operating frequencies lie in a broad band above 20 kHz for reasons of ergonomics. However, propagation of high frequency sound bears a few disadvantages, such as higher directivity and attenuation through air, as well as increased sensitivity to reflections.

As an application of a hybrid acousto-inertial tracking system, our laboratory developed a telepresence unit that allows a human user to explore virtual or remote environments by freely moving in his or her local surroundings, e.g., the living room. Video is brought to the user via a head-mounted display (HMD), position and viewing direction are determined aboard the mobile, user-worn tracking unit. Local motion is then transformed into remote movements according to a motion compression algorithm [2] that allows telepresent walking in literally unlimited spaces.

The mobile unit is integrated into a backpack containing the necessary electronics, such as a tiny computer for generating graphics as well as an embedded DSP-based board handling

signal processing for the localization task [3]. Fig. 1 shows a user walking in the telepresence environment.

For reasons of ergonomics, the entire system runs wirelessly. It is battery-operated, and communicating over WLAN and ZigBEE. The latter is required for synchronizing the mobile unit to the infrastructure, i.e., the signal generator and the beacons, to allow for performing TOF distance measurements.

A. Contribution

It is understood that NLOS distance measurements between beacons and receivers introduce a significant amount of error into pose estimation.

If not appropriately handled, they can impair the system's performance and accuracy up to total failure. Therefore, a major concern of this paper is dealing with the cause and the proper reduction or elimination of erroneous measurements. A recursive algorithm is introduced to distinguish and filter out the presumably false measurements, according to a certain quality criterion. This can be a simple χ^2 test in the deterministic case, or the mahalanobis distance, when using stochastic filtering.

Measurements are obtained concurrently between all emitters (loudspeakers) and receivers (microphones), the embedded system at the moment supports configurations of up to 8 emitters and 8 receivers. However, due to complexity issues, experiments will show setups with $4/4$ and $6/4$ emitters/receivers to better keep up with real time processing constraints.

B. Related Work

A similar approach for detecting outliers due to NLOS measurements that exploits deviations in χ^2-distribution can be found in [4]. The key idea is to determine a point position from redundant distance measurements to a higher number of beacons. After initially considering all available measurements for estimating position, in the following process the position is estimated using only subsets of the full measurement vector, in a "leave-one-out" manner. This way, when mapping back from estimated position to distances, the NLOS measurements can be discriminated according to the quadratic differences of measured and estimated distance. This approach is effective, yet computationally demanding, as it comes with $O(n!)$ complexity.

Another effective method for indoor localization under NLOS conditions that has been tested using Bluetooth and ultrasound (BLUPS) is demonstrated in [5]. It mitigates the effects introduced by NLOS measurements using a least median of squares approach.

Other approaches addressing the NLOS problem include the use of HMMs and particle filtering to keep track of the state of mobile nodes [6]. Unlike our target, they are concerned with tracking vehicles as point objects, rather than determining their pose.

C. Overview

The paper is organized as follows. The upcoming Section II formulates the problem and introduces the system modelling. Section III describes the algorithm for the NLOS discrimination. Section IV shows the hardware and the overall system design. Evaluation and sensitivity analysis can be found in Section V using synthetic data, followed by results of experiments on real data, captured by the embedded target

hardware. Section VI summarizes the results in a conclusion and motivates topics for further research.

II. PROBLEM FORMULATION

The general setup of our problem consists of a rigid body that we want to track, and a number of beacons L (loudspeakers) that are fixed at known positions within the world coordinate system. The rigid body comprises of several receivers M (microphones) that are fixed to it at known positions with respect to its local body coordinate system. Now, using the techniques presented in [7], a full number of $n \cdot m$ distances between all beacons L_i, $i = 1..n$ and all receivers M_j, $j = 1..m$ can be obtained in every update step of the measurement system. We capture these measurements in a vector called $\underline{d} \in \mathbb{R}^{n \cdot m}$

$$\underline{d} = [d_{11}, d_{12}, ..., d_{1m}, d_{21}, d_{22}, ..., d_{2m}, ..., d_{nm}]^T$$

of length $n \cdot m$. The pose of the rigid body is represented by a 12-dimensional vector, comprising of position, orientation, translational and angular velocity (each 3D). However, for the presented algorithm about static measurements, we only need the first 6 variables, i.e.

$$\underline{x} = \begin{bmatrix} \underline{p} \\ \underline{r} \end{bmatrix} ,$$

with $\underline{p} = (p_x, p_y, p_z)^T$ being the components of a 3D-position and $\underline{r} = (roll, pitch, yaw)^T$ a representation of orientation in euler angles. Its position and orientation marks the origin and the axes of the local body coordinate system.

Furthermore there is a nonlinear measurement equation that maps pose $\underline{x}$ to estimated distances $\underline{\hat{d}}$ (forward mapping),

$$\underline{\hat{d}} = \|L_{i,w} - M_{j,w}\| = \|L_{i,w} - (R \cdot M_{j,b} + \underline{p})\|$$

where R is a rotation matrix generated from $\underline{r}$. For the reverse mapping (from measured distances to estimated pose) a closed-form solution is applied, as described in [8], to serve as an initial pose estimate.

This estimate can be used for optimization by iterative methods (e.g., Newton's method) to minimize the overall error, i.e., to find a pose that minimizes the sum of squared differences between the Euklidean distance $\|[M_{i,w} - L_{j,w}]\|$ and the measurements $\underline{d}_{ij}$ for all $i, j \in i = 1..n, j = 1..m$. Thus, the microphone positions $M_{i,w}$ with respect to the world coordinate system need to be calculated by the relationship $M_{i,w} = R \cdot M_{i,b} + t$, where R is a rotation matrix, and t is a translation vector. After a number of iterations the improved estimated pose can be drawn from R and t.

The weighting for every single distance measurement d_{ij} is a component of the vector

$$\underline{w} = [w_{11}, w_{12}, ..., w_{1m}, w_{21}, w_{22}, ..., w_{2m}, ..., w_{nm}]^T$$

with $\underline{w}_{ij} \in [0, 1]^{n \cdot m}$. This enables us to gate individual measurements in or out.

Suppose now that we can solve for pose given the distance measurements. As we carry out a forward mapping, we will encounter a difference in measured distances $\underline{d}$ and those ones calculated by the mapping function, $\underline{\hat{d}}$. We now introduce a quality criterion D that reflects the deviation, by mapping the

measurement vector and the weighting vector to a scalar value $z \in \mathbb{R}^+$.

$$D : \underline{d}, \underline{w} \to z$$

For a start, we decided to take the mean squared error over all measurements involved. It is obvious that estimating the quality of the input measurements is independent of the actual pose. It merely depends on the measurements and the weighting components.

The principal challenge is now to find a configuration of $\underline{w}$ that minimizes the MSE between calculated and actual measurement, i.e., to eliminate exactly those measurements that account for an error.

$$\underline{w}_{opt} = \arg\min_{\underline{w}}\{D(\underline{w}, \underline{d})\}$$

An algorithm for recursive testing of various different configurations to approach $\underline{w}_{opt}$ is shown in Section III.

III. ALGORITHM

As stated in the previous section, the algorithm shall quantify the error introduced by certain erroneous distance measurements, and thus detect and eliminate those outliers. Prior to the recursion, an initial pose is estimated, taking the full set of measurements as an input. A weighting vector $\underline{w} = (1_{n \cdot m})^T$ qualifies for this process. This way, we receive an initial estimate consisting of pose, calculated measurements, and the mean squared error between calculated and actual measurements. Then, we descend into the recursion, operating on subsets of the given measurements, in a "leave-one-out"-manner.

The process repeats for $(n \cdot m) - 1$ times, storing the index ij of the best w-value. Now, the next step leads deeper into recursion, as again the newly calculated subsets of measurements are processed. Recursion stops once one of the following conditions is satisfied:

- The z value of calculated and actual measurements is less than a certain threshold value (required precision, one of the parameters to the algorithm)
- The least number of measurements k_{min} for full definition of 3D pose is reached (there have to be 3 residual measurements to each microphone for the pose estimation to work properly)
- The maximum recursion depth r_{max} is reached (this value is also a parameter, to keep the algorithm from locking up)

Either way, once we step out of the recursion, we get not only the estimated best pose (with hopefully all outliers removed), but also a set of useful data for further analysis, like the number of distance measurements used, and a list of all outliers, sorted by severity.

However, in severe NLOS conditions, the system can still fail to filter out all the outliers, due to the constrained minimum number of measurements needed by the closed-form solution [8] for full 3D pose estimation. The number of residual measurements k must satisfy the following inequality:

$$k \geq n \cdot dim,$$

with dim being the dimension, in our case three. [1]

---

[1]This restriction only holds for the particularly used solution where each microphone has to measure distances to at least 3 loudspeakers. In general a lesser number of measurements is sufficient for complete 3D pose definition.

Input: $\underline{d}, \underline{w}, \underline{b}, L_w, M_b, z_{max}, k_{min}, r$
1: $r = r + 1$
2: **for all** d_{ij} **do**
3:    $w_{ij} = 0$ "leave one out"
4:    solve for pose $\underline{x}$ e.g., using closed form solution in [8]
5:    calculate predicted measurement $\hat{\underline{d}}$ using measurement function
6:    calculate difference vector of predicted and actual distance measurement
7:    calculate z, e.g., the MSE of the difference above
8:    $w_{ij} = 1 \to$ reset weight to 1
9: **end for**
10: blank the index-pair ij that caused the minimum MSE by writing a 0 to $\underline{b}_{ij}$ and store the 1 permanently in $\underline{w}_{ij}$
11: calculate pose $\underline{x}$, predicted measurement $\hat{\underline{d}}$, and quality z based on the best subset (according to $\underline{b}$ and $\underline{w}$)
12: **if** $z > z_{max}$ AND $k > k_{min}$ AND $r < r_{max}$ **then**
Input: $\underline{d}, \underline{w}, \underline{b}, L_w, M_b, z_{max}, k_{min}, r$ (step down in recursion with one measurement less)
Output: $\hat{\underline{x}}, \hat{\underline{d}}, z$ (step up from recursion)
13: **end if**
Output: $\hat{\underline{x}}, \hat{\underline{d}}, z$ (end recursion)

Fig. 2.   Discriminate outliers from a set of partial NLOS measurements

The pseudo code in Fig. 2 is intended to illustrate the recursive algorithm in more detail.
Inputs are:

- $\underline{d}$ - containing $n \cdot m$ distance measurements between n loudspeakers and m microphones
- $\underline{w}$ - containing the corresponding weight components
- $\underline{b}$ - a vector $\in [0..1]^{n \cdot m}$ to blank out distances considered false
- L_w, M_b - containing geometry information (given positions $L_{w,i}$, $i = 1..n$ of loudspeakers in world coordinates and $M_{b,j}$, $j = 1..m$ microphones in body coordinates
- z_{max}, k_{min}, r - criteria for exiting recursion

Outputs are:

- $\hat{\underline{x}}$ - estimated pose
- $\hat{\underline{d}}$ - calculated (predicted) distance measurement
- z - the achieved quality (e.g., MSE)

In Section V-B the effectiveness of the above stated algorithm is demonstrated upon different emitter/receiver configurations. It runs with $O(n \cdot m)^2$ complexity.

IV. SYSTEM DESIGN

The tracking system consists of stationary infrastructure and one or more mobile units. The stationary side is made up of a number of beacons (loudspeakers) that connect to a central signal generator, shown in Fig. 3. The DSP based signal generator produces n distinguishable, unique broad band sound sequences (above 20 kHz) that are emitted by the n loudspeakers at coordinated times. The present design comprises eight channels, bearing easy scaling capability.

On the receiving side, microphones aboard the mobile, user worn unit (see Fig. 4) capture the sound in up to eight parallel buffers. A Blackfin™ DSP handles the signal processing as well as the localization tasks.
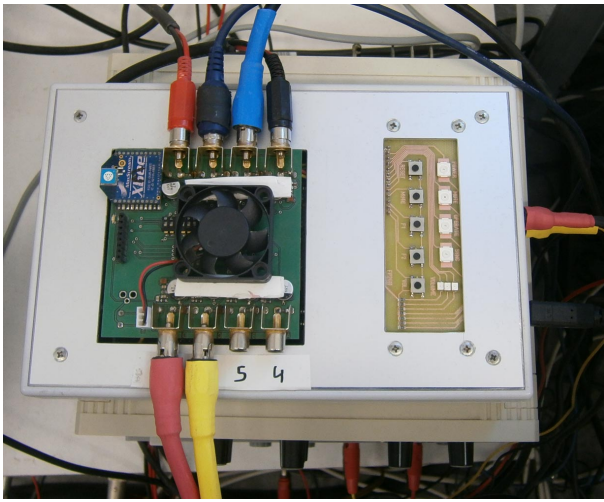
Fig. 3. The signal generator with 6 beacons attached. In the left upper corner: Radio module for synchronization with the mobile unit.

Fig. 4. A microphone array in tetrahedral shape mounted on a rail for testing. In the middle, a 3-axis-gyroscope is supplied to be fused with the acoustic tracking system. Microphones as well as the gyroscope are micro-electro-mechanical systems (MEMS).

To allow for distance measurements using the time of flight, mobile and stationary units are closely synchronized using ZigBEE[TM] radio modules.

V. Evaluation

This section opens up with a general discussion of different geometries and numbers of emitters/receivers, and how they influence measurement and pose estimation quality.

A. Sensitivity Analysis

Concluding from Time-of-Flight (TOF) measurements to positions can be considered as intersecting spheres around the emitters. Now it would be naive to think that by simply increasing the number of emitters and receivers the overall precision would increase, too. Depending on the position in a space, the intersecting angles of the spheres can get too obtuse, which leads to degradation of the position estimation.

This effect is known as geometric delusion of precision (GDOP). In order to find good, or even optimal configurations, a number of promising designs have been evaluated in Monte-Carlo-Simulations. As the minimum number of emitters/receivers for full 3D pose definition is $3/3$ (see Eq. III), the arrangement to maximize base length leads us to isosceles triangles. For configurations with more emitters/receivers (as required for reasons of redundancy in NLOS environments), tetrahedra have shown good results, as well as cubes. It seems, as if those geometric forms that maximize volume are suited best for localization, whereas planar configurations suffer from higher errors at marginal areas.

An exemplary setup of the sensitivity analysis is shown in Fig. 5. Simulated distance measurements are added a normally
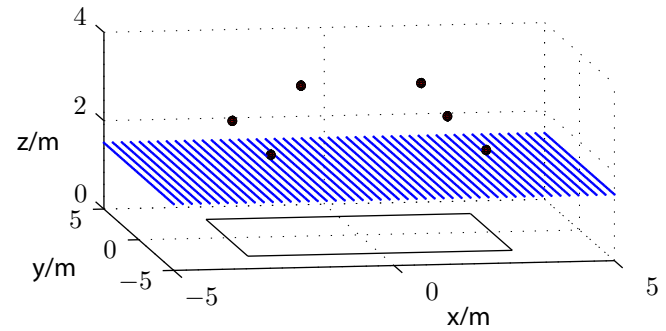

Fig. 5. The grid of microphone positions for sensitivity analysis comprises 50 lines times 50 columns to cover an area of $5 \cdot 5$ m² at a common height of 1.5 m. Six loudspeakers are mounted in a prismatic constellation, according to our actual setup.

distributed noise with $\sigma = 0.01$ m. Fig.6 shows the resulting positional standard deviation as norm over x, y and z. Fig.7 shows the standard deviation in yaw angles. Both plots show
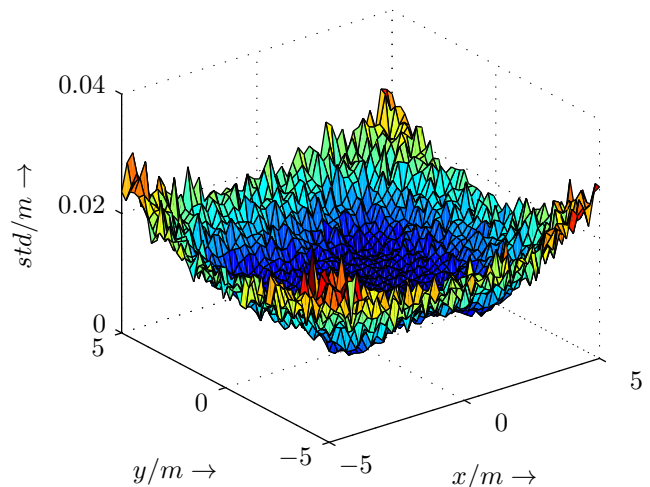

Fig. 6. Standard deviation in position as a result of a 1 cm standard deviation normally distributed noise in distances, estimated over 100 monte carlo runs per position.

that best precision is given at positions close to the center of the room, whereas estimations deteriorate when approaching marginal areas.
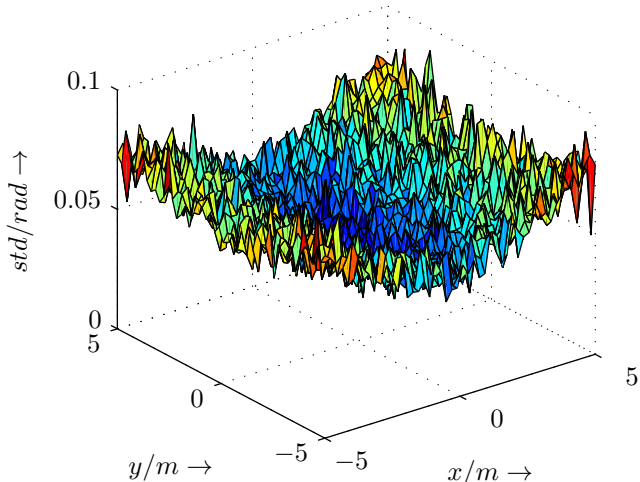
Fig. 7. Standard deviation in yaw angles as a result of a 1 cm standard deviation normally distributed noise in distances, estimated over 100 monte carlo runs per position.

B. Experiments on Real Data

The experiments performed aim at showing the influence of outliers from NLOS measurements. As a testing scenario for all the experiments, the mobile unit is mounted on a tripod equipped with a 4 meter horizontal arm, to allow for precise circular trajectories of radius 2 m. Its origin coincides with the world coordinate system's origin. Its height is fixed at 1.85 meter, also both roll and pitch angles are fixed at $0°$. Fig. 8 shows an image of the experimental setup. The rotatable arm
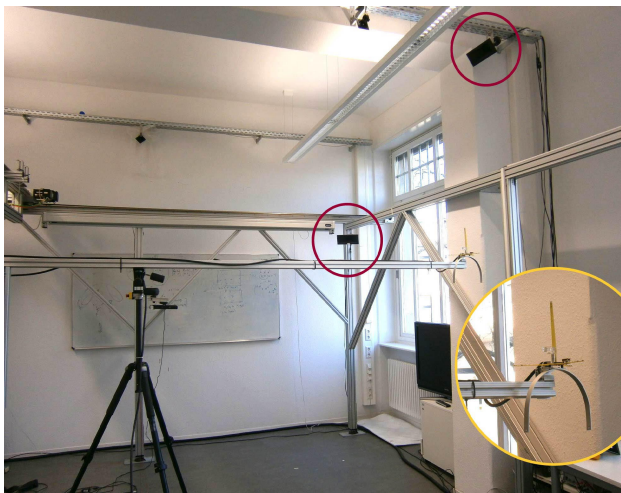
Fig. 8. The tripod is centered at the origin of the world coordinate system. The tetrahedral microphone array is mounted eccentrically by 2 m to allow for precise circular movements (see closeup at bottom). All axes are aligned to the x-y-plane using water-levels. The dark circles highlight two of the loudspeakers.

was turned by hand, so the angular rate can not be considered perfectly constant, yet, as we focus on instantaneous pose estimation, this issue can be neglected. Update rates were 10 Hz and 5 Hz for the 4/4 and 6/4 loudspeaker/microphone configuration, respectively. In both scenarios, two consecutive

circles were turned. The time to complete one circle was about 200 samples in the 10 Hz case, i.e., 20 s to cover $2\pi r \approx 12.5$ m, to imply slow walking speed.

1) Configuration: 4 *loudspeakers and* 4 *microphones:* The first experiment shows a setup of 4 loudspeakers as beacons, and 4 microphones mounted on the mobile unit. Both the beacons and the microphones are arranged to form tetrahedra. The base length (distances between microphones) is 0.2 m. As for a complete definition in 3D a minimum of 3 beacons and 3 microphones are required, this configuration leaves only little redundancy to be exploited by our algorithm.

Fig. 10 shows positions over time of the above stated scenario when all measurements are equally weighted regardless of possible outliers.
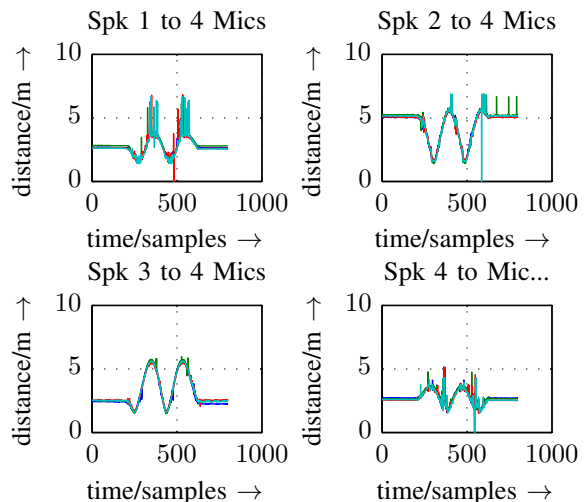

Fig. 9. The full set of distances is ordered by speaker index. Each speaker measures distances to 4 microphones. Outliers can be easily spotted by visual inspection.

The corresponding distances are shown in Fig. 9, ordered by the loudspeakers they originated from. As all the microphones are grouped within little distance, we can see that they form sine and cosine movements in the x-y-plane, according to the circular motion around the vertical (z) axis. After applying our algorithm for NLOS discrimination, the resulting trajectory can be seen in Fig. 12.

If we compare both before and after plots, we notice that the outcome is still not too satisfiable. As in some areas of the room the NLOS conditions were overwhelming, the minimum of 12 distances, given by Eq. III, was reached for several times, as shown in Fig. 11. Where the recursive algorithm clips, an untreated number of extra outliers still enters the final pose estimation. Especially for estimating the orientation, due to the small base length, these errors still lead to high deviations, which results in jittering, if transmitted unfiltered to the user's HMD.

With the most severe outliers eliminated, the results are suited for stochastic filtering. In our design, a gaussian-assumed density filter [9] is used, to dynamically fuse static (acoustic) measurements with gyroscope values, while assuming an adequate user motion model. Results are depicted in Fig. 13.
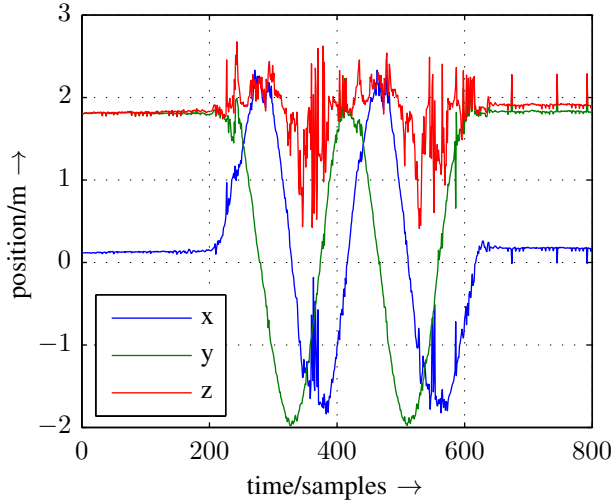
Fig. 10. Trajectory based on distance measurements from 4 loudspeakers to 4 microphones, using all 16 measurements
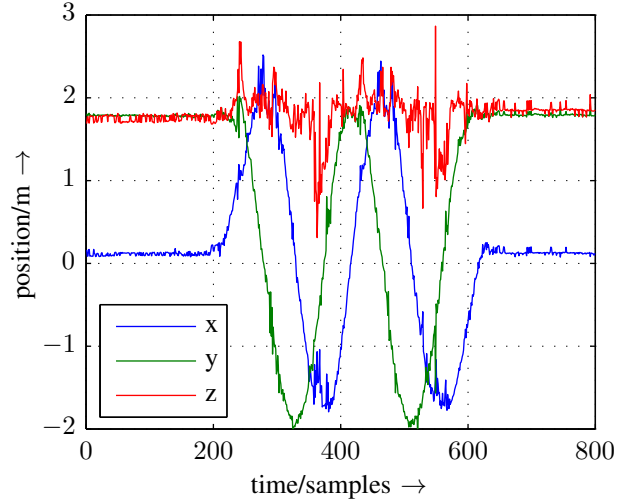

Fig. 12. Trajectory based on a subset of distance measurements from 4 loudspeakers to 4 microphones, outliers reduced by the proposed algorithm
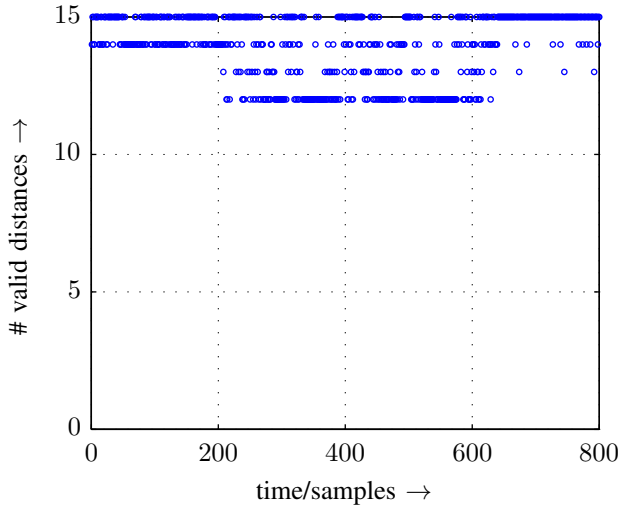

Fig. 11. Number of distance measurements chosen by the recursive algorithm for a total of $4 \cdot 4$ measurements.
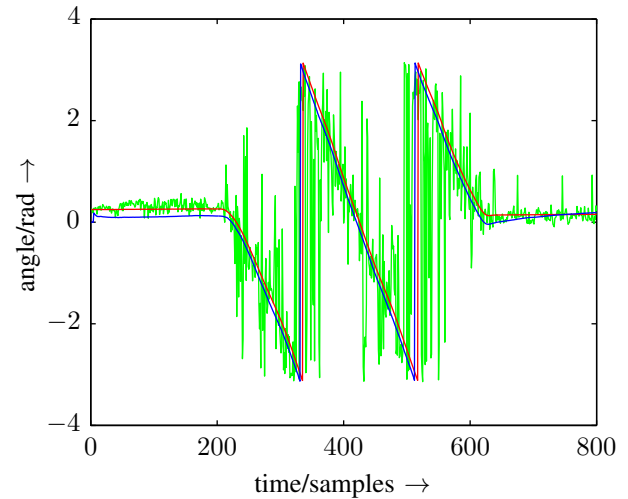

Fig. 13. Jittering yaw angle values from acoustic measurements (green) are fused with measurements from the onboard MEMS gyroscope (red) using a gaussian-assumed density filter (blue)[9]. A constant (angular-) velocity model is assumed to predict motion based on prior steps.

2) Configuration: 6 loudspeakers and 4 microphones:
Now we use higher redundancy to better cope with the overwhelming number of NLOS measurements. The corresponding measurements are all concentrated in Fig. 14. Two counterclockwise circles have been turned, Fig. 15 shows the trajectoy.

Finally, the proposed algorithm took care of most of the outliers, as can be seen in Fig. 17. Due to the short base length of 0.2 m (distance between microphones) the estimation of the orientation is very sensitive. If erroneous distances are included, the resulting angles degenerate completely. After outlier handling, the angles are in acceptable shape (see Fig. 19) to be passed to downstream fusion with gyroscope, and stochastic state estimation.

The corresponding calculated distances are shown in Fig. 16. As the number of distances used (Fig. 21) indicates, the total number of distances was still not sufficient to com-

pletely eliminate all NLOS conditions. The surroundings in our testing area mark a worst case scenario, as there are reflecting surfaces all around. The result is illustrated once more for better comparison with ground truth, which is an assumed ideal circle of 2 m radius, in Fig. 18 and Fig. 20.

VI. CONCLUSION

We have introduced a single shot pose estimation method that operates on highly redundant, partially NLOS distance measurements. The approach to select valid distances for robust outlier detection and dependable pose estimation has proven qualified for the task of indoor pose estimation, as it is required in various applications, such as telepresence systems.

Overall, in conditions with only few measurements originating from NLOS sources, accuracy is the same as in
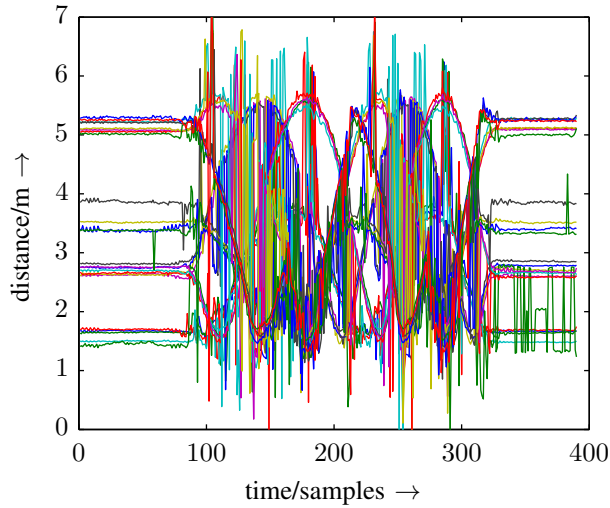
Fig. 14. Distances measured between 6 loudspeakers and 4 microphones. Visual inspection still allows us to tell the true distances from the erroneous.
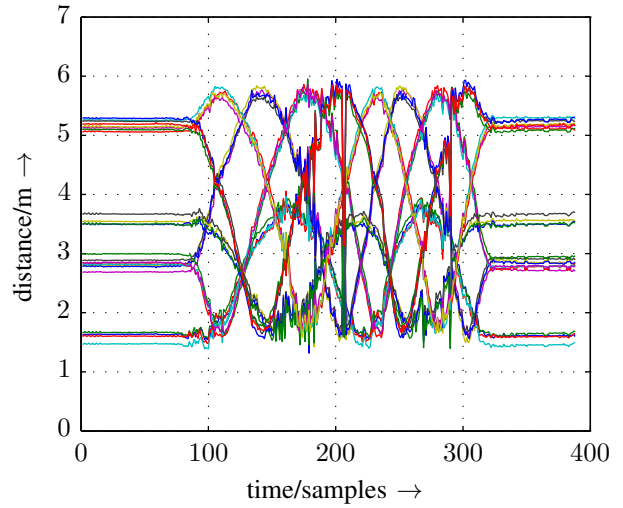

Fig. 16. Measurements calculated from the corrected pose by forward mapping.
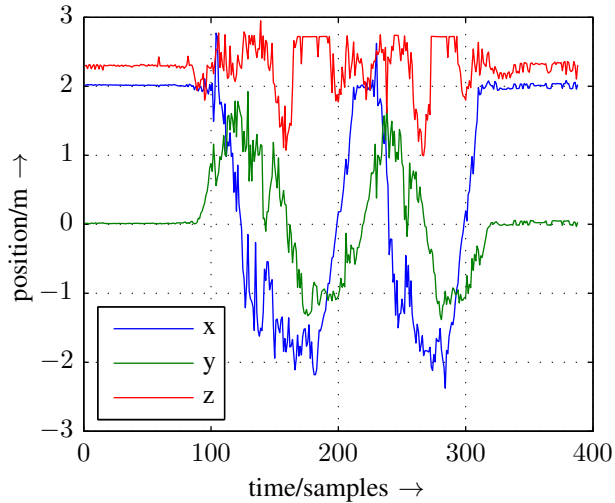

Fig. 15. Trajectory based on $6 \cdot 4$ measurements **prior to outlier handling**. Notice the false z-value perpetuating throughout the whole plot.
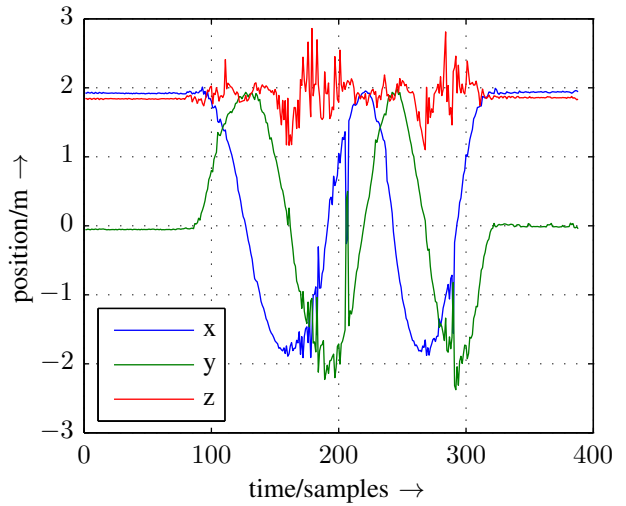

Fig. 17. Trajectory **after outlier reduction**. Complete elimination is possible, yet requires a higher redundancy in measurements, i.e., more loudspeakers/microphones.

Full-LOS-environments. In surroundings with severe NLOS conditions, the calculation complexity rises, as the search for outliers makes the algorithm descend deeper into recursion. In LOS environments, position can be resolved reliably down to centimeter range, orientation in all axes to within $5°$, depending on the base length (inter-microphone distances).

During experiments in a room of size $(5 \cdot 5 \cdot 4)$ m^3 with plenty of reflecting surfaces, such as walls, shelves, windows, and a haptic display [10] consisting of aluminum, the number of outliers could still be handled adequately by the algorithm.

Especially during initialization time robust outlier elimination is crucial, whereas during the uptime of the tracking system, localization can be supported by a gyroscope and a motion model that prevents outliers by a gating as part of stochastic state estimation.

A. Future Work

Ongoing research is concerned with improving the quality criterion deployed in the recursive outlier detection algorithm. On the way to hyper-redundancy additional knowledge, e.g., from GDOP considerations, can be exploited. Based on this notion, entire subnets of emitter/receiver pairs could be adaptively switched on and off, depending on where the best gain in information is expected. This way, exorbitant complexity can be mitigated.

As the system scales easily, hyper-redundant configurations of 50 and more microphones can be evaluated to provide guaranteed robustness and superior performance.

To overcome the limited number of loudspeakers emitting concurrently (due to bandwidth restrictions above 20 kHz), cyclic emission schemes can be evaluated.
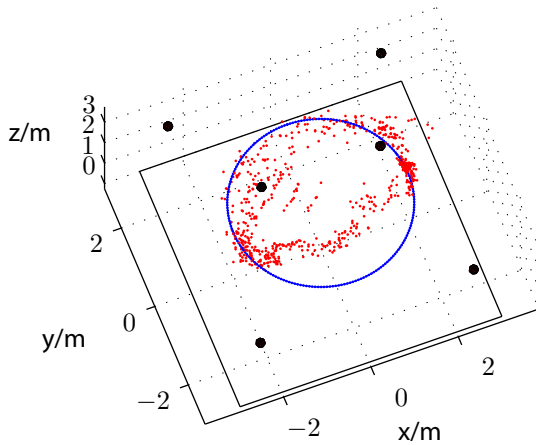
Fig. 18. Positions calculated using all measurements (**before outlier detection**), compared to ground truth (circle of 2 m radius at 1.85 m height.)
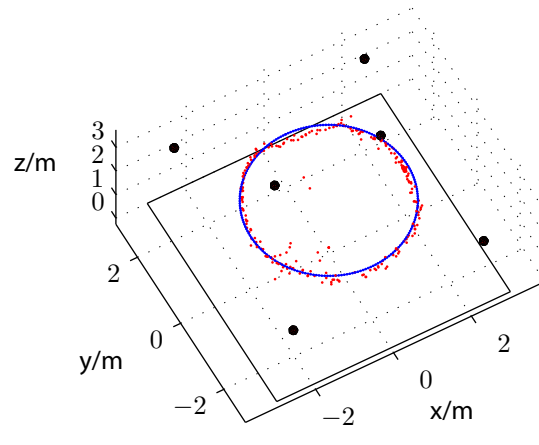

Fig. 20. Positions calculated from reduced set of measurements (**after outlier handling**), compared to ground truth (circle of 2 m radius at 1.85 m height.
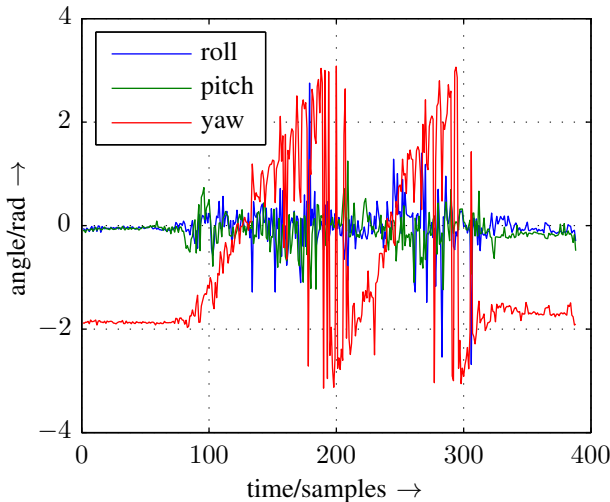

Fig. 19. Angles **after outlier handling**. The quality is sufficient to enter the dynamic stochastic filtering process (fusion with gyroscope and state prediction by system model).
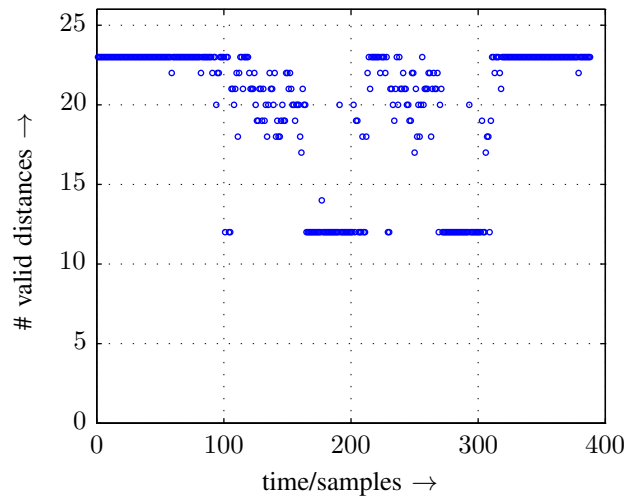

Fig. 21. Number of distance measurements chosen by the recursive algorithm from a total number of $6 \cdot 4$ measurements.

REFERENCES

[1] L. C. Mak and T. Furukawa, "A toa-based approach to nlos localization using low-frequency sound."

[2] N. Nitzsche, U. D. Hanebeck, and G. Schmidt, "Motion Compression for Telepresent Walking in Large Target Environments," *Presence: Teleoperators & Virtual Environments*, vol. 13, no. 1, pp. 44–60, Feb. 2004. [Online]. Available: http://dx.doi.org/10.1162/105474604774048225

[3] F. Packi, A. P. Arias, F. Beutler, and U. D. Hanebeck, "A Wearable System for the Wireless Experience of Extended Range Telepresence," in *Proceedings of the 2010 IEEE/RSJ International Conference on Intelligent Robots and Systems (IROS 2010)*, Taipei, Taiwan, Oct. 2010.

[4] Y.-T. Chan, W.-Y. Tsui, H.-C. So, and P. chung Ching, "Time-of-arrival based localization under nlos conditions," *Vehicular Technology, IEEE Transactions on*, vol. 55, no. 1, pp. 17 – 24, jan. 2006.

[5] R. Casas, A. Marco, J. J. Guerrero, and J. Falcó, "Robust estimator for non-line-of-sight error mitigation in indoor localization," *EURASIP J. Appl. Signal Process.*, vol. 2006, pp. 156–156, Jan. 2006. [Online]. Available: http://dx.doi.org/10.1155/ASP/2006/43429

[6] V. N. Ekambaram and K. Ramchandran, "Distributed high accuracy peer-to-peer localization in mobile multipath environments," in *Proceedings of the Global Communications Conference, 2010. GLOBECOM 2010, 6-10 December 2010, Miami, Florida, USA*. IEEE, 2010, pp. 1–5.

[7] F. Packi, F. Beutler, and U. D. Hanebeck, "Wireless Acoustic Tracking for Extended Range Telepresence," in *Proceedings of the 2010 IEEE International Conference on Indoor Positioning and Indoor Navigation (IPIN 2010)*, Zürich, Switzerland, Sep. 2010.

[8] F. Beutler and U. D. Hanebeck, "Closed-Form Range-Based Posture Estimation Based on Decoupling Translation and Orientation," in *Proceedings of the 2005 IEEE International Conference on Acoustics, Speech, and Signal Processing (ICASSP 2005)*, vol. 4, Philadelphia, Pennsylvania, USA, Mar. 2005, pp. 989–992.

[9] M. F. Huber and U. D. Hanebeck, "Gaussian Filter based on Deterministic Sampling for High Quality Nonlinear Estimation," in *Proceedings of the 17th IFAC World Congress (IFAC 2008)*, vol. 17, no. 2, Seoul, Republic of Korea, Jul. 2008.

[10] P. Rößler, T. Armstrong, O. Hessel, M. Mende, and U. D. Hanebeck, "A Novel Haptic Interface for Free Locomotion in Extended Range Telepresence Scenarios," in *Proceedings of the 3rd International Conference on Informatics in Control, Automation and Robotics (ICINCO 2006)*, Setúbal, Portugal, Aug. 2006, pp. 148–153.